

# Microbial formation of a halloysite-like mineral

メタデータ	言語: eng
	出版者:
	公開日: 2017-10-03
	キーワード (Ja):
	キーワード (En):
	作成者:
	メールアドレス:
	所属:
URL	<a href="https://doi.org/10.24517/00010585">https://doi.org/10.24517/00010585</a>

This work is licensed under a Creative Commons  
Attribution-NonCommercial-ShareAlike 3.0  
International License.



**Title page**

**Manuscript title: MICROBIAL FORMATION OF A  
HALLOYSITE-LIKE MINERAL**

Author; KAZUE TAZAKI

Address of institutions of authors: Department of Earth Sciences, Faculty of Science,  
Kanazawa University, Kakuma, Kanazawa, Ishikawa 920-1192 Japan

**Running title: Microbial halloysite**

**Mailing address: KAZUE TAZAKI**

**Address of institutions of author: Department of Earth Sciences, Faculty of  
Science, Kanazawa University, Kakuma, Kanazawa, Ishikawa 920-1192 Japan**

**E-mail address: [kazuet@kenroku.kanazawa-u.ac.jp](mailto:kazuet@kenroku.kanazawa-u.ac.jp)**

**Phone: 81-76-264-5736**

**FAX: 81-76-264-5746**

# MICROBIAL FORMATION OF A HALLOYSITE-LIKE MINERAL

KAZUE TAZAKI

Department of Earth Sciences, Faculty of Science, Kanazawa University, Kakuma,  
Kanazawa, Ishikawa 920-1192 Japan

**Abstract**--Transmission electron microscopy demonstrated the biological formation of a hollow spherical halloysite-like mineral in freshwater systems. The interaction between clays and microbes was investigated in microbial films from laboratory cultures derived from natural sediments. Optical and electron microscopic observations of cultured microbes revealed that thin clay films covered areas of the bacterial cell wall. XRD of the thin films after two years of aging showed a  $7.13 \text{ \AA}$  *d*-spacing, consistent with a  $7 \text{ \AA}$  halloysite-like phase  $[\text{Al}_2\text{Si}_2\text{O}_5(\text{OH})_4 \cdot \text{H}_2\text{O}]$ . FT-IR analysis of the thin film exhibited the characteristic adsorption bands for O-H ( $3651 \text{ cm}^{-1}$ ), C-H and C-N ( $2925$ ,  $1454$  and  $1420 \text{ cm}^{-1}$ ), suggesting that the phase was closely associated with adhesive organics. TEM observation of the thin films revealed that spherical, hollow halloysite-like material formed on both coccus and bacillus type bacterial cells. Electron diffraction analysis of this material showed  $2.9$ ,  $2.5$ ,  $2.2$  and  $1.5 \text{ \AA}$  *d*-spacings. The present investigation strongly suggests that the thin film wall of the spherical halloysite-like material was associated with bacteria as a bio-organic product. This material, hereafter called bio-halloysite, is more evidence for the microbially mediated

formation of clay minerals. The identity of the bacteria responsible for bio-halloysite formation is unknown, but is tentatively assigned to sulfate-reducing bacteria on the basis of morphology and the presence of reducing conditions in the microcosm at the end of the experiments.

**Key Words**—microbial formation, halloysite, hollow spherical forms, bacterial cell wall, electron microscope

## INTRODUCTION

Soils are dynamic systems showing a variety of energy and mass fluxes and material transformations, and various models have been proposed to describe the formation of clay minerals within soils. Upper layers of a soil have high organic carbon concentrations and organic content decreases with increasing depth in the soil. This gradient is usually thought to be due to the dominance of above-ground organic input to the carbon profile and much lower activity of organisms in the soil itself (Shoji, et al., 1993). However, the major formation processes for clay minerals are thought to be biochemical, largely depending on high microbial activity in soils (Ueshima and Tazaki, 1998; Ueshima et al., 2000).

Examples of clay-biochemical interactions abound. Hanczyc et al. (2003) reported that the clay montmorillonite catalyzes the polymerization of RNA from activated ribosome nucleotide and that montmorillonite accelerates the spontaneous conversion of fatty acid micelles into vesicles. Theng and Orchard (1995) discussed the physical and chemical

interaction between microorganisms and soils in the ecosystems. Bio-mineralization of kaolinite, nontronite, and bentonite on living cells of microorganism in natural and cultivated systems have been reported (Tazaki, 1997; Ueshima et al, 2000; Asada and Tazaki, 2000; Tazaki, 2000). The degree of mineralization in these examples ranged from poorly crystalline granules to well oriented crystalline solids. Polymeric substances secreted by microbial cells including the crystalline surface (i.e., S-) layer proteins, polysaccharides, and capsules often provide nucleation sites and possibly a favorable chemical microenvironment for bio-mineral formation. Bacterial cells can act as a nucleation site for minerals (Ferris et al., 1986; Sara and Sleytr, 2000). Similarly, Tashiro and Tazaki (1999) showed that the layer of extracellular polymeric substances surrounding microbial cells can act as a template in the formation of iron hydroxides. Urrutia and Beveridge (1993) suggested a cation bridging mechanism in which multivalent metal cations complex with a functional group (e.g. COO-) that in turn bridges with ionic silicates to form large aggregates. Theng and Orchard (1995) also suggested that multivalent cations might have served as cation bridges in the interaction between clays and microbial extracellular polymeric substances.

In this study, natural occurrences of clay minerals in freshwater systems have been observed at nano-meter to micro-meter scales using electron microscopy. Laboratory cultivation experiments clarified the role of microbes in clay biomineralization. We observed that hollow spherical mineral forms became encapsulated on the active surface of the cell wall and that hollow spheres of a 7 Å-halloysite-like phase, hereafter termed bio-halloysite, were produced by bacteria in natural freshwater lake sediments at room temperature. We also discuss the mechanism of formation of this phase on bacterial

surfaces and suggest that this morphology develops due to either outgassing or vesicle formation. Study of these small-scale “clay bubbles” can also contribute to a better understanding of the proposed environments for the development of the earliest forms of life, associated with bio-sedimentation on Earth.

## **MATERIAL AND METHODS**

Sediment samples were collected from Passo Real Dam sediments, Portalegre, Brazil (Fonseca et al., 2000; Tazaki and Asada, 2003). Twenty grams of reddish brown sediment, composed mainly of kaolinite with quartz, cristobalite, and feldspar, were rinsed with distilled water ten times to remove fine particles. The washed sediments were incubated at room temperature under distilled water in a covered beaker with a glass slide oriented as shown in Fig. 1. The incubation periods ranged from a few months to 2 years, during which time the pH, Eh, and DO (Dissolved Oxygen) of the solution in the beaker were measured using a HORIBA portable inspection meter.

Microbes in the biofilms were examined with a polarizing optical and fluorescence microscope (Nikon OPTIPHOT-2 EFD3) using wet samples. Two fluorometric methods were used for bacteria counting. Samples stained with 4', 6-diamidino-2-phenylindole (DAPI) were observed through an episcopic fluorescence microscope. DAPI stains the DNA in bacterial cells, and blue fluorescence under ultraviolet light (365 nm) indicates metabolically active bacteria. Samples stained with 0.1 mM 5-carboxyfluorescein diacetate (CFDA) were used for counting enzymatically active bacteria. These samples were incubated for microscopic observation.

A low-vacuum scanning electron microscope (LV-SEM, JEOL JSM-5200LV) equipped with an energy dispersive X-ray (EDX) spectrometer (Philips EDAX PV9800EX) was used to observe the micromorphology of the bacterial surface and its chemical composition. Microbial films were mounted on stubs using carbon tape and air-dried. Dehydrated samples were coated with carbon and examined at accelerating voltages of 15-25 kV.

The extracellular and intracellular condition of the bacteria were observed using TEM (JEOL JEM-2000 EX). Electron diffraction analysis was used to identify phases present in the biofilms. One drop of the suspension was taken by pipette and mounted on the micro-grid for observation. The accelerating voltage ranged between 120 and 200 kV.

Mineralogical investigations of clay-bio-film aggregates were performed by X-ray powder diffraction (XRD). A Rigaku Rinto 1200 X-ray diffractometer (CuK<sub>α</sub> radiation) operating at 40 kV and 30 mA, and a scanning speed of 1 - 20 sec./0.02 degree, was used. Chemical investigations of the bio-films were carried out by X-ray fluorescence using a scanning electron microscope (SEM) equipped with an energy dispersive X-ray fluorescence detector (ED-XRF, JEOL JSX-3201; Rh-K<sub>α</sub>-ray). Both bio-films and powdered samples were investigated using the LV-SEM and TEM (operated at an acceleration voltage less than 120kV).

The organic compounds associated with minerals and organometallic complexes in the biofilm were analyzed by Fourier-transform infrared absorbance spectroscopy (FT-IR; Jasco FT/IR-610, MICRO-20). The biofilm was air-dried and ground to a fine powder, 3 μg of powdered microbial films and 10 mg of amorphous potassium bromide

(KBr) were placed in a mortar, mixed thoroughly, and made into tablets using an MP-1 micro tablet maker and an MT-1 model mini-press. FT-IR analysis was then carried out on the tablets using IR frequencies between 400 and 4000cm<sup>-1</sup>.

## RESULTS

Analysis of the untreated sediments (dispersed on Mylar film) by ED-XRF showed that they contained large amounts of Si, Al, and Fe, with traces of Na, Mg, K, Ca, Ti, and Mn. Analysis by XRD of the initial sediment showed that no halloysite-like phase was present in the untreated sediments, yet it did contain kaolinite. Micro morphology by optical microscopy confirmed no hollow spheres in the initial stage. After two years, the dissolved constituents in the water were analyzed by ED-XRF and contained 23 ppm Fe and 16 ppm Si associated with C, Na, Mg, Al, P, S, K, and Ca ions, suggesting some sediment dissolution and transformation had occurred.

Biofilms were observed on the glass surface after a few months, and grew to 0.01 to 0.1 mm thick after one year. Biofilms formed not only on the glass slide, beaker, and top surface of the sediments, but also were apparent as an oily film on the surface of the solution (Fig. 1). No biofilms grew in control samples that had been sterilized either by ultraviolet rays after boiling for 3 hours or by the use of ethanol instead of distilled water.

The biofilms were coated with newly formed clays after a few months aging at room temperature. The solution and the biofilms turned brown in color after 2 years of aging, suggesting the precipitation of a mixture of Fe oxides and sulfides (probably iron-sulfide). A sulfide odor suggested the presence of H<sub>2</sub>S gas in the system. The

slightly reduced redox state of the solution was confirmed by Eh values of  $-26\text{mV}$  and dissolved oxygen levels of  $1.3\text{ mg/l}$  at pH 7.4.

### **Optical and fluorescence microscopic observations**

After two years, the biofilms were mainly composed of colonies of spherical brown or greenish brown microbes associated with filamentous microbes. Optical micrographs showed abundant microbes associated with brown clay particles after 2 years of aging (Figure 2A). The microbes fluoresced red when exposed to light of 510-560 nm wavelength, indicating that the microbes contain chlorophyll-a, which has absorption bands at 409 and 665 nm (Figure 2B). The various microbes were tentatively identified on the basis of their morphologies (Holt et al., 1994) as filamentous algae ( $1.5 - 2\text{ }\mu\text{m}$  in width), spherical algae ( $1 - 10\text{ }\mu\text{m}$  in diameter), Cyanobacteria ( $2\text{ }\mu\text{m}$  in width), and bacteria having coccoid or bacillus morphology ( $<1\text{ }\mu\text{m}$  in width). The size of spherical cells ranged from  $< 1$  to  $10\text{ }\mu\text{m}$  in diameter (Figure 2). Filamentous algae and the coccoid/bacilloid bacteria (possibly sulfate-reducing bacteria) were the primary producers of spherules. Filamentous algae produced larger spherules (See Figure 2) than the coccoid/bacilloid bacteria (See Figures 5 and 6), for which spherules could only be seen by TEM magnification.

### **X-ray diffraction and Energy dispersive X-ray fluorescence analyses**

Wet biofilms from the 2 month culture were mounted on a ceramic tile and measured as wet samples. The XRD patterns of the biofilms showed a rounded peak at  $7.20\text{ }\text{\AA}$ , suggesting the presence of  $7\text{ }\text{\AA}$  clay minerals (Fig. 3 top). On the other hand, wet biofilms from the 2 year old culture showed peaks at  $7.13\text{ }\text{\AA}$ (001),  $4.43\text{ }\text{\AA}$ (02),  $3.55\text{ }\text{\AA}$

(002), 2.49 Å (200), 2.36 Å (003), 2.22 Å (04), 1.68 Å (24) and 1.48 Å (06) (Fig. 3, bottom). The XRD criteria for halloysite given by Dixon (1989) based on the relative intensities of the 0.445-nm and 0.7-nm XRD reflections. The 0.7-nm phase in Fig. 3 is kaolinite, but the morphological characteristics are consistent with spherical halloysite-like phase to call it “bio-halloysite”. Traces of quartz and cristobalite were also found (Fig. 3, bottom). No evidence for feldspar was seen, suggesting that it had dissolved during the 2 years of aging. The *d*-spacing of the newly formed clay was the same as that of kaolin group clay minerals, such as kaolinite or meta-halloysite. The high background in the upper pattern suggested the presence of organic materials. The chemical and mineralogical components of the bacteria show chemical bonds with Si-O, Al-OH and organics, based on ED-XRF and FT-IR data (Figs. 4 and 7).

ED-XRF analysis of the culture solution (Figure 4A) and cultured bioorganic clay (Figure 4B), exhibited abundant Al, Si, S, K, Ca, Ti, Mn and Fe associated with traces of C, Mg, and P. These elements might be derived from the dissolution of sediments included feldspars. The enrichment of S and Fe over other elements are recognized in bio-halloysite bearing biofilms. No FeS<sub>x</sub> minerals were identified, The FeS<sub>x</sub> minerals could be of very low crystallinity and hence not seen by diffraction. Microorganisms, such as bacilli and cocci in the SEM of Figure 4, are encased in exopolymeric substance. Arrows indicate broken hollow clay bubbles, due to the vacuum in the SEM specimen chamber. The chemistry and *d*-spacing of the halloysite-like phase obtained by XRD and SEM agreed with the electron diffraction data obtained by TEM.

#### **Low vacuum scanning electron microscope (LV-SEM) and transmission electron**

### **microscope (TEM) observations**

Optical micrographs of the biofilms clearly showed abundant filamentous bacteria associated with spherules (Figure 2). Scanning electron micrographs of biofilm showed smaller bacteria with hollow clay spherules 1-5  $\mu$  m in diameter (Figure 4 arrows). Abundant coccus and bacillus type bacteria were also observed on the surface of the biofilms. Chemical analysis was carried out on different parts of the biofilm. In most cases three elements (Al, Si, and Fe) were detected in the wall of the hollow spherules, whereas additional S was detected in the bacterial cell (Figure 4B). The EDX spectra of bacteria indicated that the most abundant elements were Al, Si, S, and Fe and the high background suggested the presence of organic materials, whereas EDX analyses of matrix around the bacteria showed a low background of organics.

TEM images of hollow spherules, about 1  $\mu$  m in diameter, show different stages spherule growth, with darker marginal areas (indicating higher electron density than in the center) that strongly suggest spherical halloysite (Figures 5 and 6). These hollow spherules grew to 1 to 10  $\mu$  m in diameter after shorter aging times such as 2 months. The inner parts appear amorphous, nearly transparent in the TEM image (Figures 6A and B). The thin outer skin of Figures 6A and B seems to thicken to eventually produce a dense mass of halloysite-like material as in Figures 5B and 6C. Electron diffraction spots at 2.5, 2.2, and 1.5 Å and XRD reflections at 4.43 Å(02), 2.56 Å(20), 2.49 Å(003), 2.22 Å(04), and 1.48 Å(06) are similar to those expected for 7-Å-halloysite and kaolinite. The 2.9 Å *d*-spacing might be due to the presence of maghemite 2.95 Å(220) or magnetite 2.97 Å(220), because XRF data (Figure 4) also showed high Fe content.

The mineral assemblage probably contained small amounts of ferrihydrite.

Our observations revealed that the thin skin of bio-halloysite spherules thickens to eventually form bio-halloysite spheres. Sudo and Shimoda (1978) and Sudo et al. (1980) have reviewed the formation of spherical halloysite in weathered volcanic ash soils in Japan. The micro morphology and the size of spherical halloysite in their study are very similar to the bio-halloysite in this study.

TEM observations clearly showed that spherical bio-halloysite is associated with the surface of bacteria (Fig. 5). The development of spherical halloysite from a thin hollow sphere to a thick-walled spherical form is shown in Figure 6. Some of the hollow spheres were broken out as shown in Figure 6B. The diameter of clay bubbles increased with length of aging. Therefore, the optical micrographs collected after 2 years of aging (Fig. 2) show the clay bubbles having a minimum diameter of  $5\ \mu\text{m}$ , whereas TEM micrographs collected after shorter aging times such as 2 months (Figures 5 and 6) show the clay bubbles of 500 nm in diameter.

### **FT-IR spectra**

The FT-IR spectrum of bio-halloysite showed a wide range of bands at 3750–3550  $\text{cm}^{-1}$  (O-H stretch), and 1500–1300  $\text{cm}^{-1}$  (C-N-H combination) associated with prominent absorption bands at 3697, 3622, 3405 (O-H), and 1657  $\text{cm}^{-1}$  ( $\text{H}_2\text{O}$ ). The C-H stretch (2925  $\text{cm}^{-1}$ ), Si-O stretch (1034  $\text{cm}^{-1}$ ), Al-OH stretch (912  $\text{cm}^{-1}$ ) and Si-O stretch (537 and 471  $\text{cm}^{-1}$ ) were identified as bio-halloysite (Fig. 7). The most likely explanation was that the 3651  $\text{cm}^{-1}$  absorption band was derived from bio-halloysite. The 1454 and 1420  $\text{cm}^{-1}$  (C-N stretch) was also recognized as organics, because the

standard kaolinite (API62, Cornwall, UK) did not show these bands. The other peaks were mainly from the organic matter of microorganisms, such as N-H, C-H, C=O, and C-N-H stretches derived from nucleic acids, fatty acids, and polypeptides (Filip and Hermann, 2001), whereas the Si-O and Al-OH bands are derived from clay spherules.

The FT-IR spectrum of bio-films showed bands characteristic of organics in contrast to the sediment samples. The absorption band at  $1100\text{ cm}^{-1}$  was likely due to organic P-O. Either nucleic acids or cell-wall and capsular lipids containing polysaccharides, could be responsible for these features. The cell proteins were typically indicated by a number of amide bands (Filip and Hermann, 2001).

Bio-halloysite has therefore been shown to be a mixture of a  $7\text{ \AA}$ - halloysite-like phase and bioorganic products through the mineralogical, chemical, and biological measurements described above.

## **DISCUSSION**

### *Biomining of halloysite on microbes at pH 6-7*

Halloysite is a common constituent in volcanic-derived soils and occurs as the dominant clay mineral in many Si-rich environments. Halloysite has a 1:1 aluminum:silicon ratio, and exhibits diverse morphologies, such as tubular and spheroidal forms. Most commonly, halloysite has a 1.0 nm basal spacing, with two interlayer water molecules per formula unit. However, halloysite is susceptible to dehydration, which leads to a 0.7 nm basal spacing.

In this study, bio-halloysite was successfully formed from the dissolution of kaolinite or feldspars in a cultivated biofilm after a few months and 2 years of aging at room

temperature. Electron microscopic observations revealed that bio-halloysite grew as a thin film on the cell wall of bacillus type bacteria. The thin films of bio-halloysite are inflated at the cell wall to form a hollow spherical form similar to that found in volcanic ash soils.

Halloysite exhibits a wide range of structural disorders due to random stacking of structural layers. Wada and Kakuto (1985) described a poorly crystalline form of halloysite that they termed embryonic halloysite. These materials showed no X-ray diffraction peaks but exhibited infrared absorption bands characteristic of halloysite. In this study, FT-IR data of bio-halloysite showed spectral bands at 3697 and 3622  $\text{cm}^{-1}$  suggesting the characteristic O-H bond of structural water (Tazaki and Asada, 2003). The strong bands at 2925 and 1454 are labeled as being due to C-H stretching and bending vibrations. The presence of a mixture of OH<sub>2</sub> and OH<sub>4</sub> absorptions were recognized (Bish and Johnston, 1993). The absorption bands at 1454 and 1420  $\text{cm}^{-1}$  were due to abundant organic materials in halloysite (Fialips et al., 2000).

Hanczye et al. (2003) present experimental simulations of how clay formation may have operated and been linked with proto-life. They show that simple physicochemical forces can drive growth and division, and that mineral particles, such as clays, can catalyze the assembly of vesicles in water. The mineral particles must have a high surface charge to be able to nucleate lipid vesicles from a solution of micelles (Russell, 2003).

The cell wall of a microbe is covered with organic adhesive material, including polysaccharides that might organize the formation of oriented clusters associated with clay particles (Ueshima and Tazaki, 2001). Kennedy et al. (2002) reported that organic

carbon controls the orientation of mineral surfaces in black shales. Therefore, clay mineral formation by bacteria is linked with the adhesive nature of surface materials that leads to inflated spherules or “clay bubbles”.

*Comparison with spherical halloysite in volcanic soils* Spherical halloysite is often found in volcanic soils, ashes and altered pumice beds. These halloysites commonly have a high Fe content, but little or no S. For comparative purposes, a rock, consisting mainly (ca. 90%) of K-feldspar, was collected from Ilha Bela, Southern Brazil. A thick reddish rind on the rock contains well-developed gibbsite and tubular halloysite (Figure 8B) formed under extreme leaching conditions (Tazaki and Fyfe, 1987a, 1987b). Energy dispersive XRF analysis of the circular materials on the K-feldspar shows that it consists of Si and Fe with small amounts of Al, K, and Mn (Figure 8B inset). Further alteration shows 7 Å lattice images and circular primitive sheet structures reminiscent of globular halloysite (Figure 8A). Fe-rich compositions are typical of spherical halloysite (Kirkman, 1977). As shown in Figure 8B clay precursors may well precede the formation of spherical particles of halloysite, although they have not been described as the result of biologically mediated alteration

In the present study, a spherical halloysite-like phase having a high S content formed with the mediation of microorganisms under reducing conditions. The biomineralization of halloysite correlated with sulfate reduction and H<sub>2</sub>S gas production. Aerobic conditions are necessary for the initial breakdown of hydrocarbons and in subsequent steps, nitrate or sulfate may serve as a terminal electron acceptor (Bartha, 1986). The low Eh and dissolved oxygen values observed in this experiment suggest that reducing conditions were present, and that sulfate-reducing bacteria may have played a

role in the formation of bio-halloysite.

#### *Formation mechanism of bio-halloysite*

Based on the current evidence, one can only speculate as to the formation mechanism of the bio-halloysite. One such mechanism is proposed in Fig. 9. I suggest that bacteria inflate a thin clay skin to form a vesicle through some form of degassing, probably of the  $O_2$ ,  $CO_2$  or  $H_2S$  gases which accumulated in the culture solution, on the basis of morphology, the presence of reducing conditions, a high S content and the odor. If the algae or cyanobacteria are involved in the formation of bio-halloysite, then  $O_2$ , and/or  $CO_2$  gases produce the hollow spheres. If only coccoid/bacilloidal bacteria are associated with the bio-halloysite,  $H_2S$  gas could be involved. The pH changed during the course of experiment, from pH 6 at the starting point to pH of 7.4 after 2 years of aging. The composition of the solution also changed, Al, Si, and Fe all increased.  $H_2S$  gas was generated and the solution smelled of sulfur as the redox status of the solution changed, with the Eh dropping to 0-50 mV. This suggests the presence of sulfate-reducing bacteria, as these would generate copious amounts of  $H_2S$  (g) and would precipitate Fe as a sulfide. The bacteria observed in this study facilitated the bioorganic formation of the clays. The cell walls of microbes generally include polysaccharides and proteins, and have an affinity for clay minerals. The vesicles were pushed out from the adhesion surface at the cell wall as the microbe generated and released gases. This leads to the uniform size and bubble morphology of the clay. The rate of gas generation must be constant and the cell pore size must be uniform to result in the relatively uniform size of the clay bubbles.

A contrasting model is based on the assumption that no free gas can be found in

bacteria unless they have special organelles, called “ gas vesicles”, to separate the gas from the fluid phase in the cytoplasm. Any gas produced internally would therefore be dissolved and would diffuse out of the cell. Gram-negative bacteria normally produce and liberate vesicles from their surface (Beveridge, 1999). No gas is necessary to “blow” these “bubbles” since they are naturally excised from the bacterium. The vesicles consist of outer membrane and periplasmic materials and make good nucleation sites for mineral development. Most sulfate reducing bacteria are gram-negative bacteria.

Synthesis in NaCl brines designed to simulate crystallization of rounded particles has been demonstrated (Goldman and Stoffers, 2002). Similar rounded phases ( $\text{Si/Fe} = 0.26$ ) were synthesized under saline, neutral, hydrothermal conditions ( $40^\circ\text{C}$ , pH7, 2M NaCl, with initial  $\text{Si/Fe} = 1.5$ ). This resulted in poorly ordered hisingerite, exhibiting a very broad XRD pattern , and having an oval morphology arranged in very fine sheets. In my study the phase did not resemble hisingerite, instead it produced a new bio-halloysite phase suggesting the key role played by the microbes.

In this study, the laboratory experiments indicated that bio-halloysite formation in fresh water after a few months to 2 years of aging can be ascribed to an initial crystallization of biological origin, rather than inorganic origin. Clay bubbles may have initially produced by bacterial degassing or vesicle formation. Clay bubbles of a uniform size form intervals on the cell wall structure (Figure 9). Some of clay bubbles were fragile and easily broken due to the thin wall (Figure 4 and Figure 6B). Hollow spheres developed as shown by the decreasing density from the rim to the center of the bubble. With time the thin films thicken, becoming a dense wall as shown in Figure 6C. Finally, the well-crystallized halloysite-like clay bubbles (vesicles) might have been released

from bacterial surface to the external environment, cutting off all contact with the bacterial cell. These clay bubbles might serve as a precursor for spherical halloysite crystallization. However, I argue that the major halloysite nucleation processes are biochemical, largely depending on high microbial activity in soils. The observation that microbial cells could mediate the formation of halloysite-like phases is a significant one that should have important consequences for the soil sciences.

## CONCLUSION

TEM micrographs clearly showed the biological formation of primitive clay bubbles and the growth of a transitional product of spherical bio-halloysite. The clay bubbles, 1  $\mu$  m in diameter, occurred as hollow spherical forms on the surfaces of bacterial cells. The chemical analysis of the clay bubbles showed Al, Si, S, and Fe as the major elemental composition. The electron diffraction pattern also identified the spheres as a halloysite-like phase. X-ray diffraction, FT-IR spectroscopy, ED-XRF, and SEM-EDX analytical methods used in this study suggested that the clay bubbles did not resemble hisingerite or other clay minerals, but represented a new ordered iron-aluminum silicate phase, hereafter called bio-halloysite. The clay bubbles might serve as a precursor for spherical halloysite crystallization. This shows that microbial activity may play a significant role in the nucleation of clays, and that this may be a common occurrence. It is likely that the clay bubbles on the surface of bacterial cells are the bioorganic product of bacterial degassing or vesicle formation activity. Halloysite-like mineral formation in a soil may be substantially enhanced by the presence of bacteria.

## ACKNOWLEDGMENTS

My thanks to Dr. Jim Amonette and Dr. David Dettman for their constructive comments and helpful suggestions on ways to improve this manuscript, and to Dr. Masayuki Okuno and Dr. Ryuji Asada for their technical assistance. This study was partially supported by Grant-in-Aid for Science Research from the Ministry of Education, Science, and Culture, Japan (Grant-in-Aid for Scientific Research B).

## REFERENCES

- Asada, R. and Tazaki, K. (2000) Observation of bio-kaolinite clusters. *Clay Science Japan*, **40**, 24-37.
- Bartha, R.(1986) Biotechnology of petroleum pollutant biodegradation. *Microbial. Ecol.*, **12**, 155-172.
- Beveridge, T.J. (1999) Structures of gram-negative cell walls and their derived membrane vesicles. *J. Bacteriology*, **181**, 4725-4733.
- Bish, D.L. and Johnston, C.T. (1993) Rietveld structural refinement of dickite at 12 K. *Clays and Clay Minerals*, **41**, 297-304.
- Dixon, J. B. (1989) Kaolin and serpentine group minerals. p. 467-525 *In* J. B. Dixon and S. B. Weed (eds.) *Minerals in Soil Environments*, 2<sup>nd</sup> ed., SSSA Book Series 1, Soil Science Society of America, Madison, WI.
- Ferris, F.G., Beveridge, T.G. and Fyfe, W.S. (1986) Iron-silica crystallite nucleation by

bacteria in geothermal sediment. *Nature*, **320**, 609-611.

Filip, Z. and Hermann, S. (2001) A attempt to differentiate *Pseudomonas* spp. and other soil bacteria by FT-IR spectroscopy. *European Journal of Soil Biology*, **37**, 137-143.

Fialips, C-I., Petit, S., Decarreau, A., and Beaufort, D. (2000) Influence of synthesis pH on the kaolinite crystallinity and surface properties. *Clays and Clay Minerals*, **48**, 173-184.

Fonseca, R., Barriga, F., Fyfe, W.S., and Tazaki, K. (2000) A geological study of bottom sediments from Passo Real and Capingui reservoirs, Rio Grande do Sul, Brazil. *Abstract of International Geological Congress, Rio, Brazil*, 235.

Hanczyc, M.M., Fujikawa, S.M., and Szostak, J.W. (2003) Experimental models of primitive cellular compartments: Encapsulation, growth, and division. *Science*, October 24, **302**, 618-622.

Holt, J.G., Krieg, N.R., Sneath, P.H.A., Staley, J.T. and Williams, S.T. (1994) Bergey's manual of determinative bacteriology. Ninth Edition, Williams & Wilkins, USA, pp787.

Kennedy, M.J., Pevear, D.R. and Hill, R.J. (2002) Mineral surface control of organic carbon in black shale. *Science*, **295**, 657-660.

Kirkman, J.H. (1977) Possible structure of halloysite disks and cylinders observed in some New Zealand rhyolitic tephra. *Clay Minerals*, **12**, 199-216.

Russell, M.J. (2003) The importance of being alkaline. *Science*, October 24, **302**, 580-581.

Sara, M. and Sleytr, U.B. (2000) S-layer proteins. *J. of Bacteriology*, **182**, 859-868.

Shoji, S., Nanzyo, M. and Dahlgren, R.A. (1993) Volcanic ash soils: Genesis, properties, and utilization. Elsevier, Netherlands. 288pp.

- Sudo, T. and Shimoda, S. (1978) Clays and clay minerals of Japan: Developments in Sedimentology 26, Elsevier. 300pp.
- Tashiro, Y. and Tazaki, K. (1999) The primitive stage of microbial mats comprising iron hydroxides. *Earth Science*, **53**, 27-35.
- Tazaki, K. (1986) Observation of primitive clay precursors during microcline weathering. *Contrib. Mineral. Petrol.* **92**, 86-88.
- Tazaki, K. and Fyfe, W.S. (1987a) Formation of primitive clay precursors on K-feldspar under extreme leaching conditions. *Proceedings of the International Clay Conference, Denver, 1985*, 53-58.
- Tazaki, K. and Fyfe, W.S. (1987b) Primitive clay precursors formed on feldspar. *Canadian Journal Earth Science*, **24**, 506-527.
- Tazaki, K. (1997) Biomineralization of layer silicates and hydrated Fe/Mn oxides in microbial mats: An electron microscopical study. *Clays and Clay Minerals*, **45**, 203-212.
- Tazaki, K. (2000) Formation of banded iron-manganese structures by natural microbial communities. *Clays and Clay Minerals*, **48**, 511-520.
- Tazaki, K. and Asada, R. (2003) Microbes associated with clay minerals; Formation of bio-halloysite. In: 2001. A Clay Odyssey, E.A. Dominguez, G.R. Mas, and F. Cravero (Eds.), Elsevier, Amsterdam, Netherlands, 569-576.
- Theng, B.K.G. and Orchard, V.A. (1995) Interactions of clays with microorganisms and bacterial survival in soil: A physicochemical perspective. Environmental impact of soil component interactions, P.M. Huang, J. Berthelin, J.M. Bollag, W.B. McGill and A.L. Page (eds.), CRC press, Florida, 3, 123-139.

- Ueshima, U., Mogi, K. and Tazaki, K. (2000) Microbes associated with bentonite. *Clay Science Japan*, **39**, 171-183.
- Ueshima, M. and Tazaki, K. (1998) Bacterial bio-weathering of K-feldspar and biotite in granite. *Clay Science Japan*, **38**, 68-82.
- Ueshima, M. and Tazaki, K. (2001) Possible role of microbial polysaccharides in nontronite formation. *Clays and Clay Minerals*, **49**, 292-299.
- Urrutia, M.M. and Beveridge, T.J. (1993) Mechanism of silicate binding to the bacterial cell wall in *Bacillus subtilis*. *Journal of Bacteriology*, **175**, 1936-1945.
- Wada, K. and Kakuto, Y. (1985) Embryonic halloysites in Ecuadorian soils derived from volcanic ash. *Soil Science Soc. American J.* **49**, 1309-1318.

## Captions

Figure 1. A schematic diagram of the simple culture system shows formation of biofilms on a glass slide, a wall of covered bottle, and surface of sediments in distilled water at pH of 6-7 and in sunlight.

Figure 2. Optical micrographs of biofilm showing abundant microorganisms associated with clay particles.

A; optical micrograph of spherical materials (arrow heads) associated with filamentous algae, spherical algae, cyanobacteria and filamentous bacteria,

B; fluorescence micrograph of a DAPI-stained sample shows the red fluorescence of

chlorophyll-a in spherical cells and in filamentous algae (arrows).

Figure 3. XRD pattern of biofilms after 2 months and 2 years of aging, showing the progressive crystallization of bio-halloysite.

Figure 4. Low vacuum scanning electron micrograph of bio-film with ED-XRF analyses of dried culture-solution (A) and biofilm (B). The EDX spectrum of living filamentous bacteria showed major elements Al, Si, S, and Fe (B). The Rh peak is due to X-ray tube. Arrows indicate broken hollow clay bubbles, due to vacuum in the SEM specimen chamber.

Figure 5. Transmission electron micrographs of bio-halloysite in clay bubbles on the surface of bacillus type bacteria (A). The electron diffraction pattern with 2.9, 2.5, 2.2 and 1.5 Å<sup>-1</sup> spacing also supports the mineralogical evidence of a 7 Å<sup>-1</sup> halloysite-like mineral (B, inset).

Figure 6. Transmission electron micrographs of development of bio-7 Å<sup>-1</sup> halloysite of clay bubbles. The thin wall of the bio-halloysite bubble (A) thickens to form a dense halloysite sphere (C). Some of the clay bubbles were broken out to form hollow cavities (B). The diameter increases from 800 nm to about 1 μm during aging.

Figure 7. FT-IR spectroscopy of clay bubbles in biofilms, showing not only Si-O and Al-O bands due to clay minerals, but also various kinds of organic bands, such as fatty

acids, nucleic acids, and polypeptides (Filip and Hermann, 2001).

Figure 8. Transmission electron micrograph of the well-developed spherical halloysite in volcanic ash soils from Mt. Daisen (A) and the well-developed primitive clay precursors on K-feldspar (B) showing a 15-20 nm circular form and 1.4 - 2.0 nm lattice images. Energy dispersive analysis of the material in (B) which consists of Al, Si, K, Mn, and Fe (inset). The Cu peak is due to the micro grid.

Figure 9. Schematic diagram illustrating one possible mechanism of clay bubble bio-halloysite formation. These clay bubbles might serve as a precursor for spherical halloysite crystallization. The formation mechanism of the hollow sphere morphology of bio-halloysite seems to be the inflation of clay bubbles by the degassing of H<sub>2</sub>S gas into the cohesive materials of the bacterial cell wall under the low redox condition of the solution.

Revised manuscript on 29<sup>th</sup> December 2004

New title: Microbial formation of a halloysite-like mineral

24<sup>th</sup> April 2004 SUBMISSIONS OFFICE of CLAYS AND CLAY MINERALS  
Editor-in-Chief  
Derek C. Brain and Dr. Amonette

Dear Prof. Brain and Dr. Amonette

I would like to send my revised manuscript, according suggestion by Dr. Amonette. :

Title <Microbial formation of halloysite > by Kazue Tazaki.

Enclosed please find the copy of the revised manuscript where changes have been made.  
Dr David Dettman (The University of Arizona) improved English on this manuscript.

I send also the revised manuscript electronically as a single Adobe. Pdf file (including text, references, captions and figures.

The manuscript has not been published, is not currently submitted for publication elsewhere, wholly, or in part, nor will be submitted elsewhere while in the review process for CLAYS AND CLAY MINERALS.

Contributions may be (1) papers on original research.

Enclosed please find an original and three copies.

Yours sincerely,

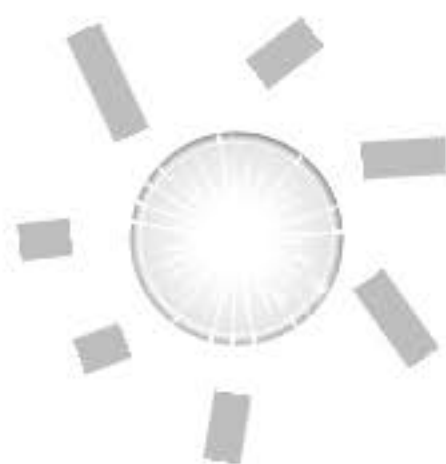
Kazue Tazaki

Department of Earth Sciences, Faculty of Science, Kanazawa University, Kakuma,  
Kanazawa, Ishikawa 920-1192 Japan

E-mail; kazueta@kenroku.kanazawa-u.ac.jp

Phone; 81-76-264-5736

Fax; 81-76-264-5746



filter paper

pH meter  
Eh meter

biofilms

pH 6.0 → 7.4  
water

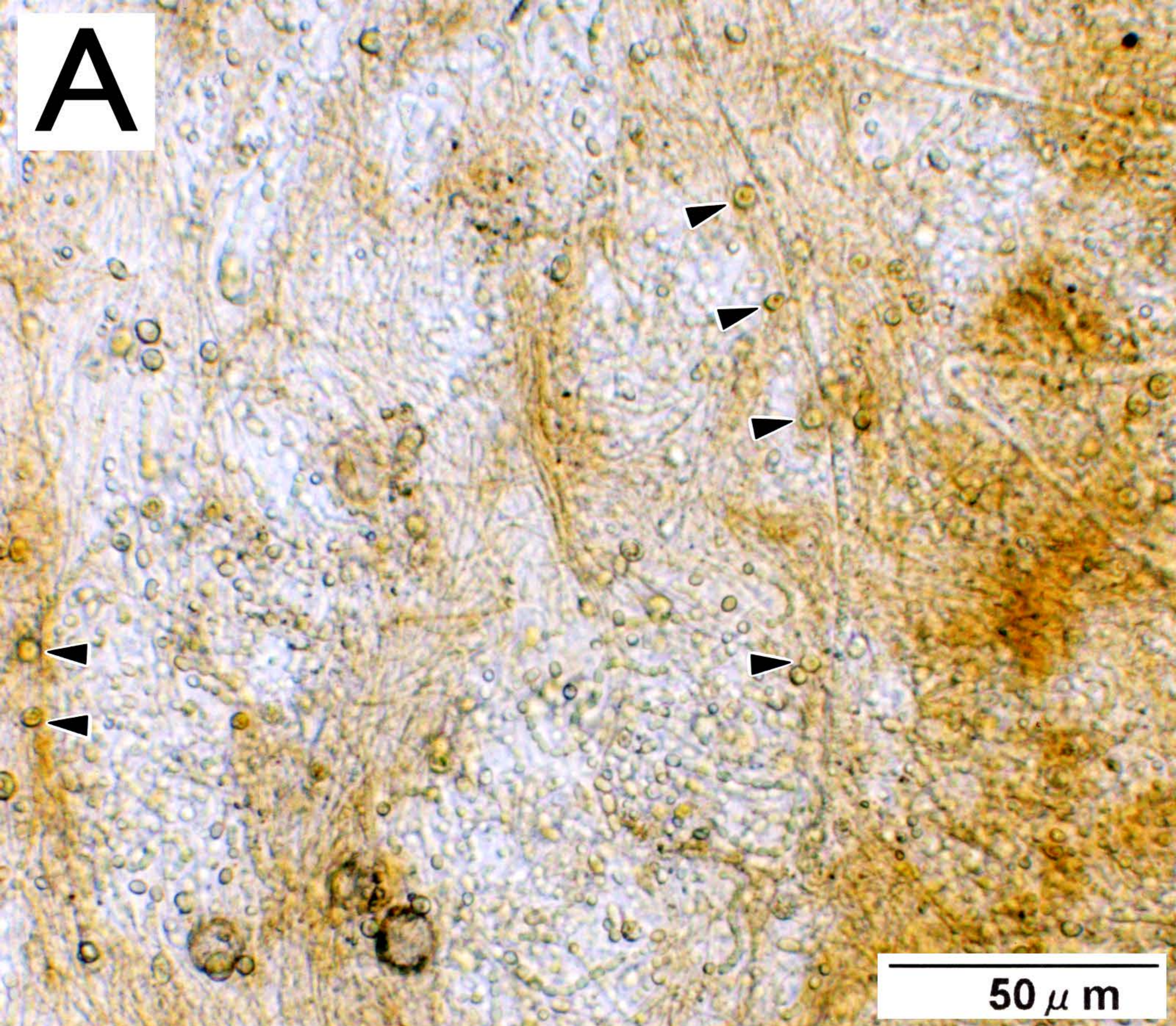
glass slide

biofilms

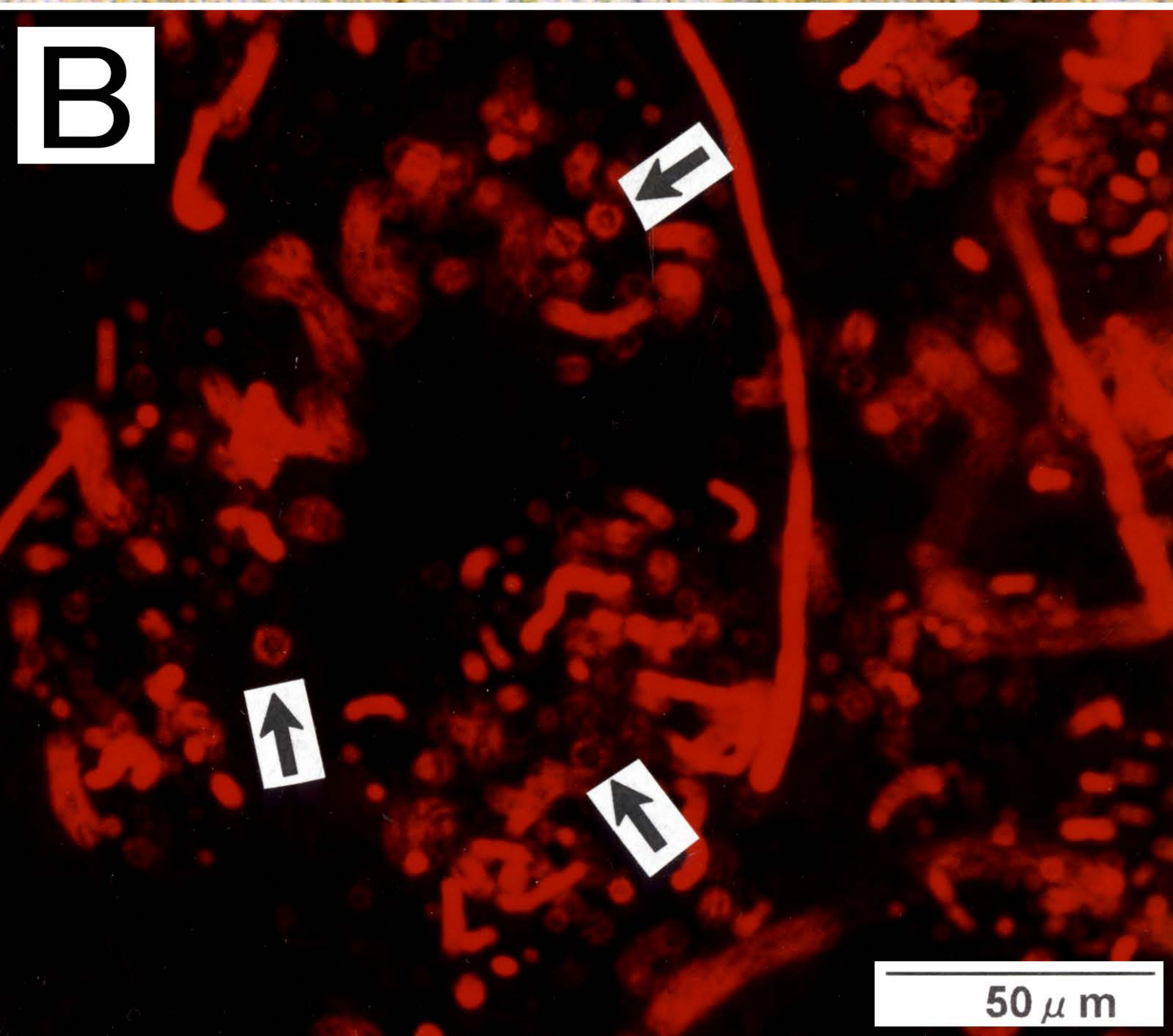
sediments

5 cm

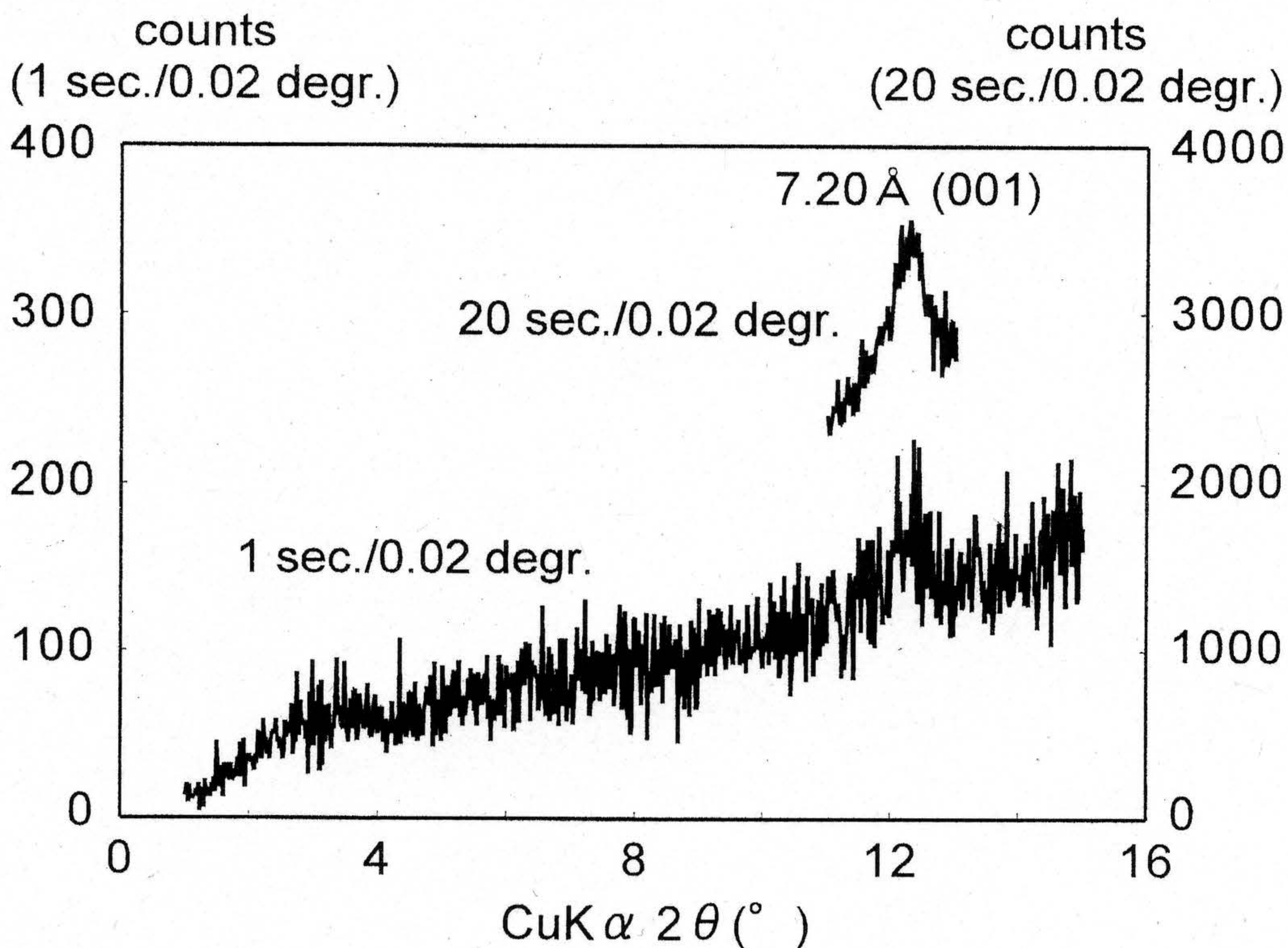
**A**



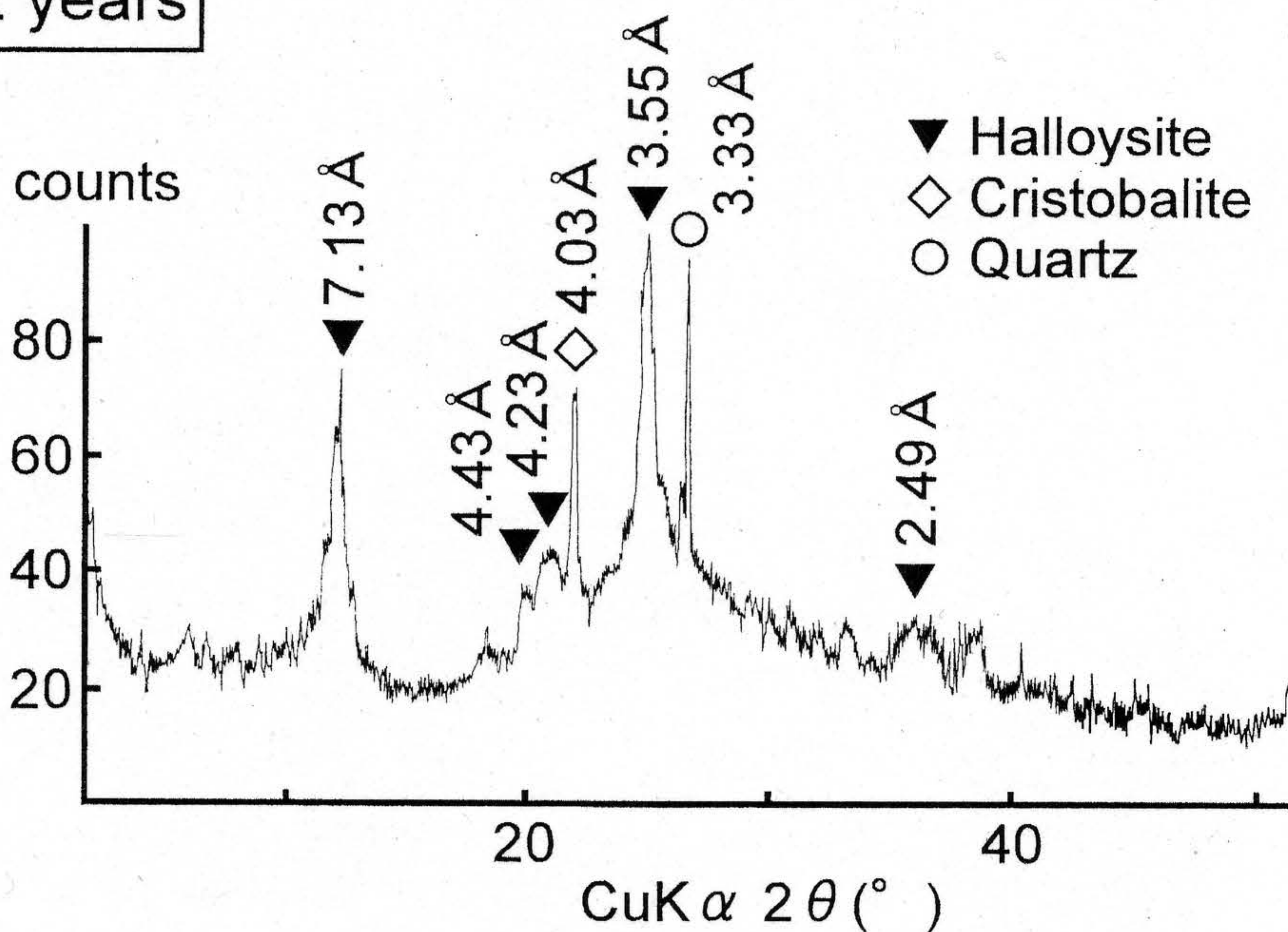
**B**

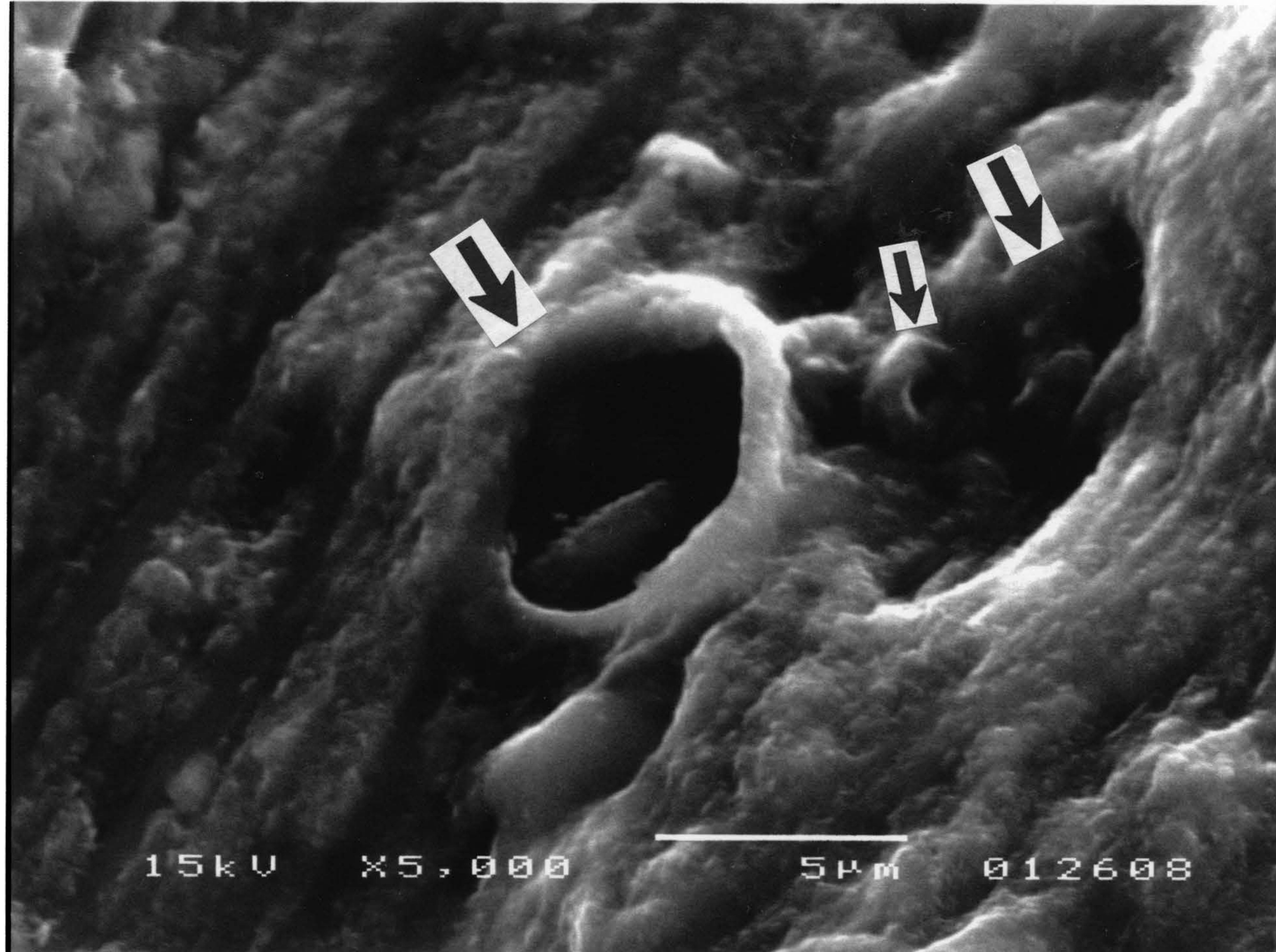


2 months

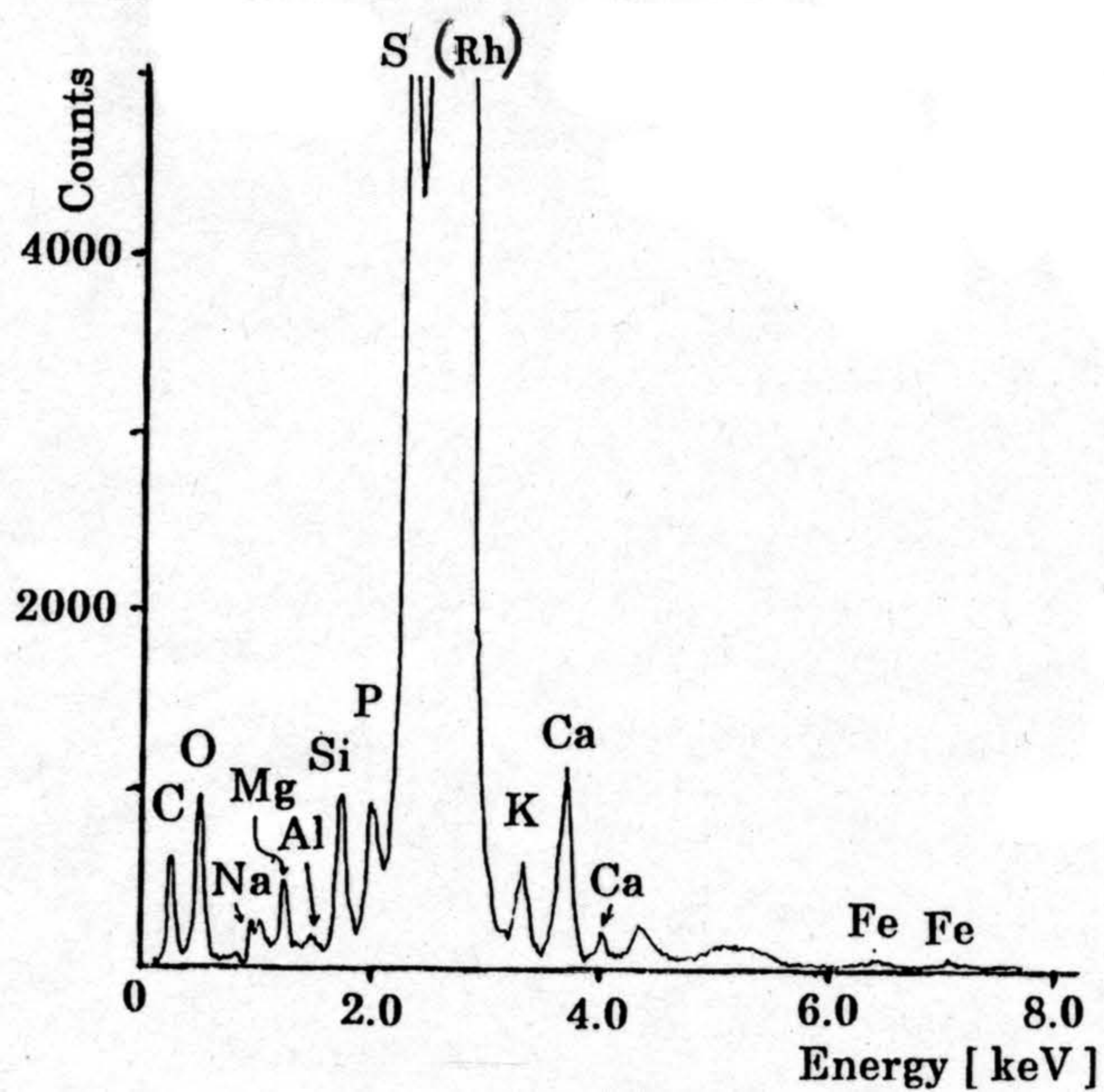


2 years

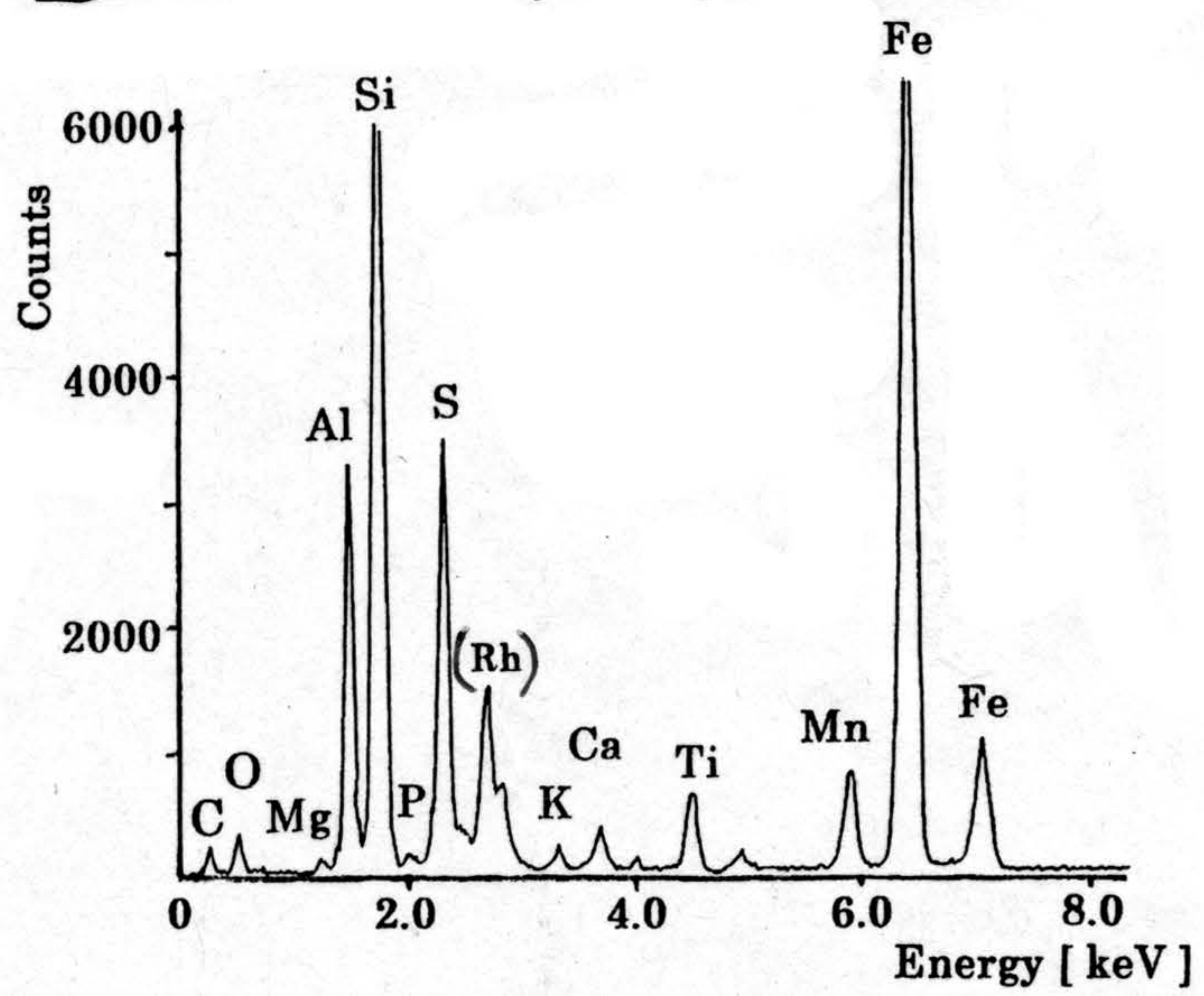




## A Culture solution



## B Bio- Halloysite(Biofilm)



**A**

Halloysite

Bacterium

500 nm

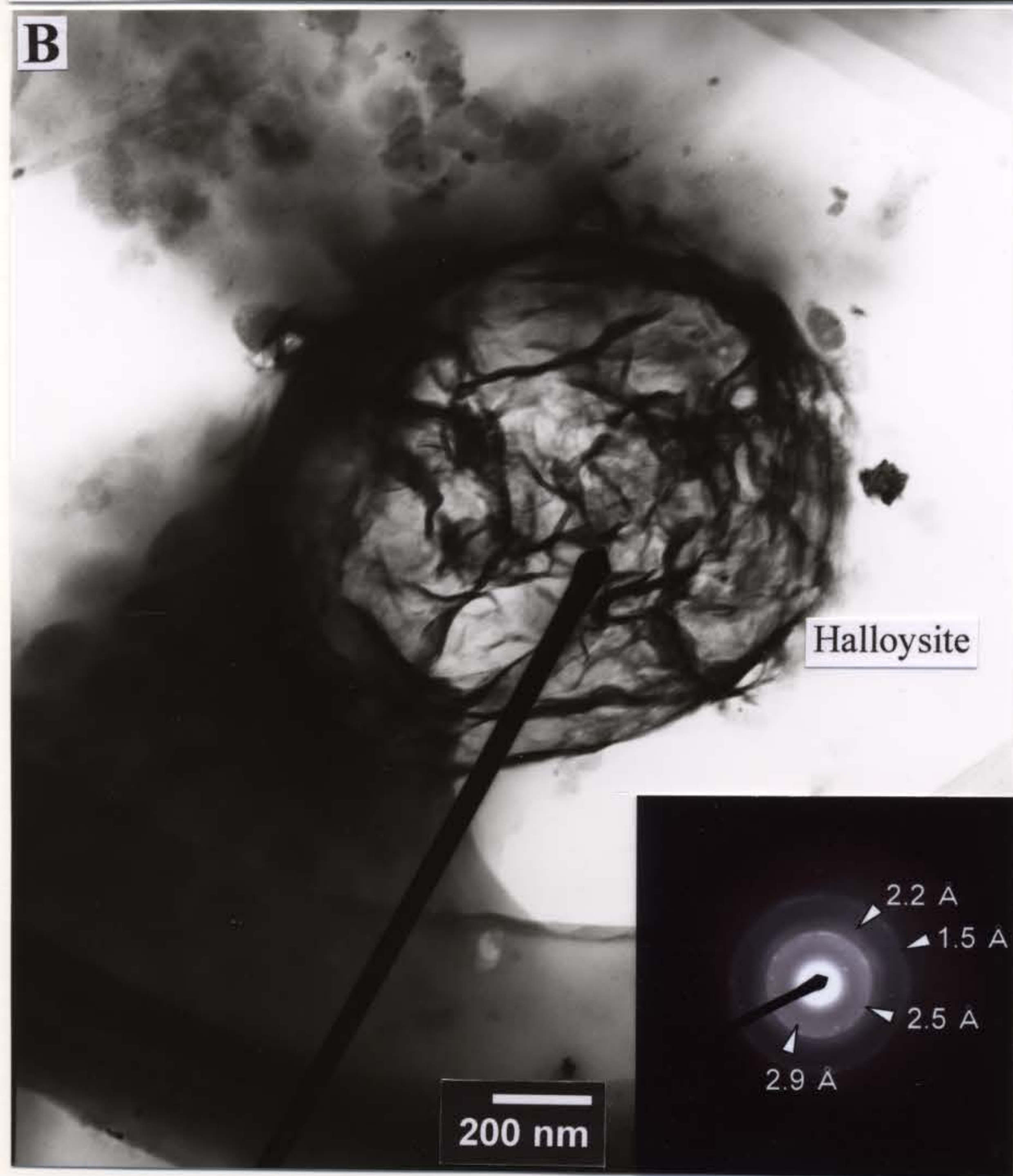
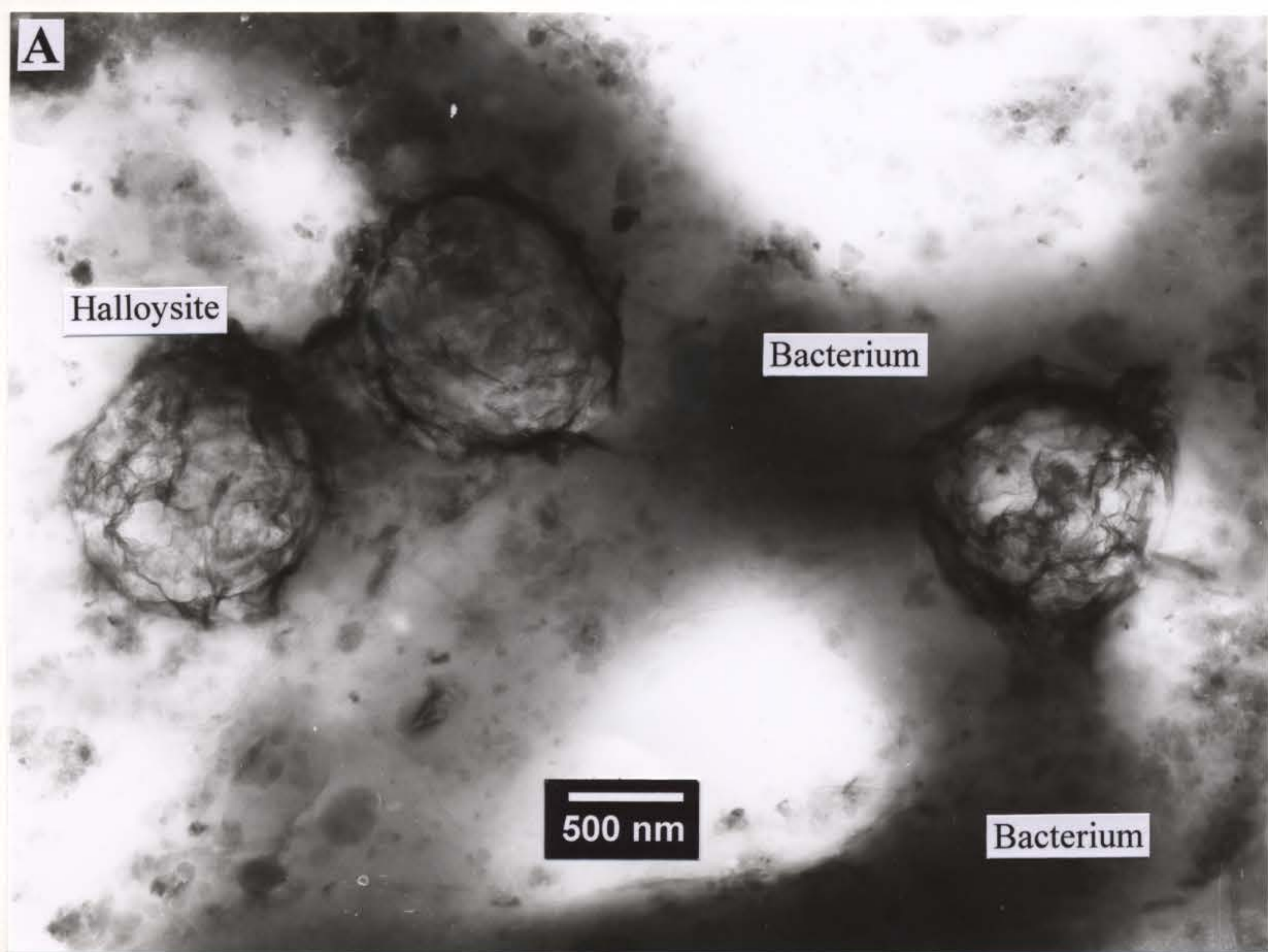
Bacterium

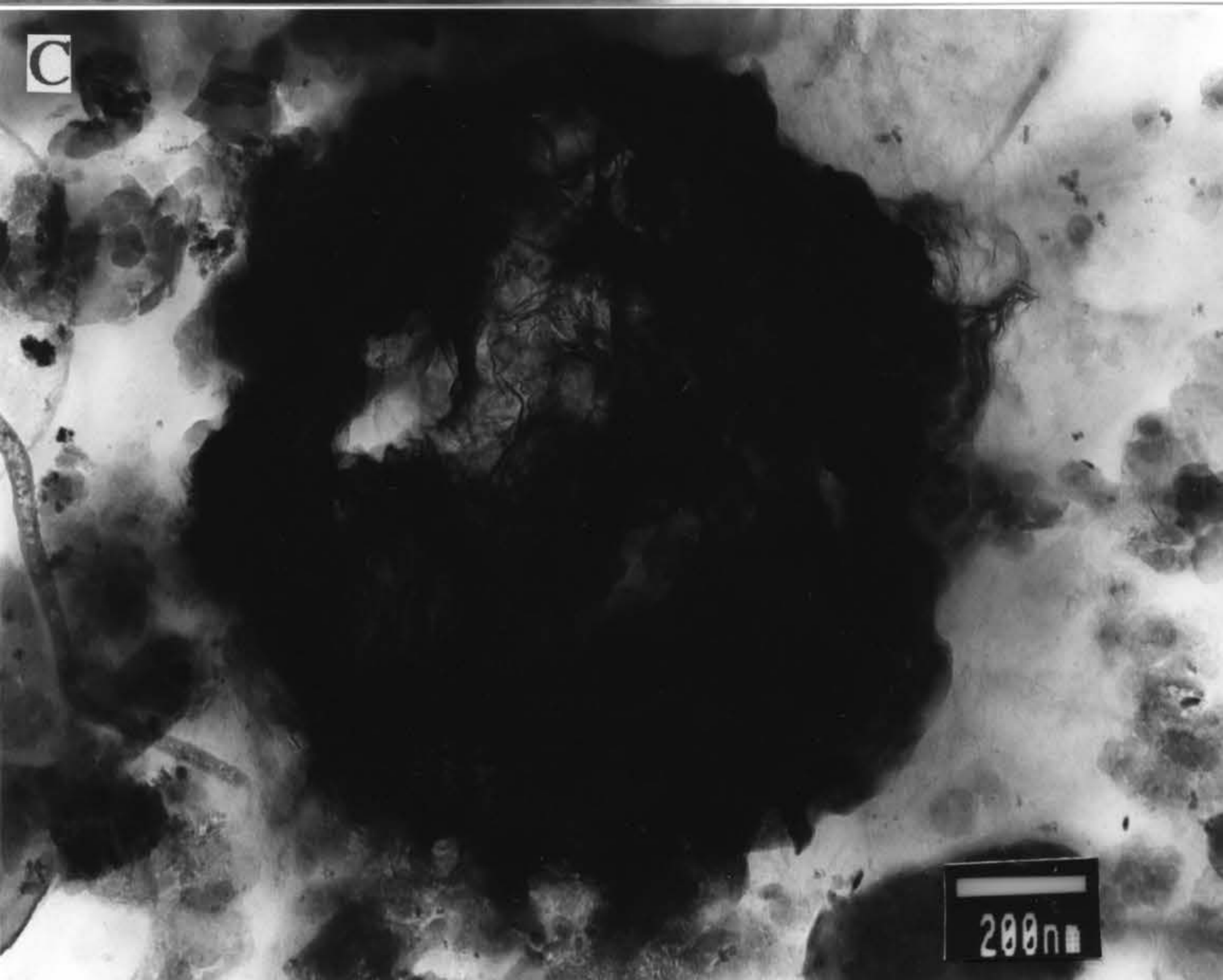
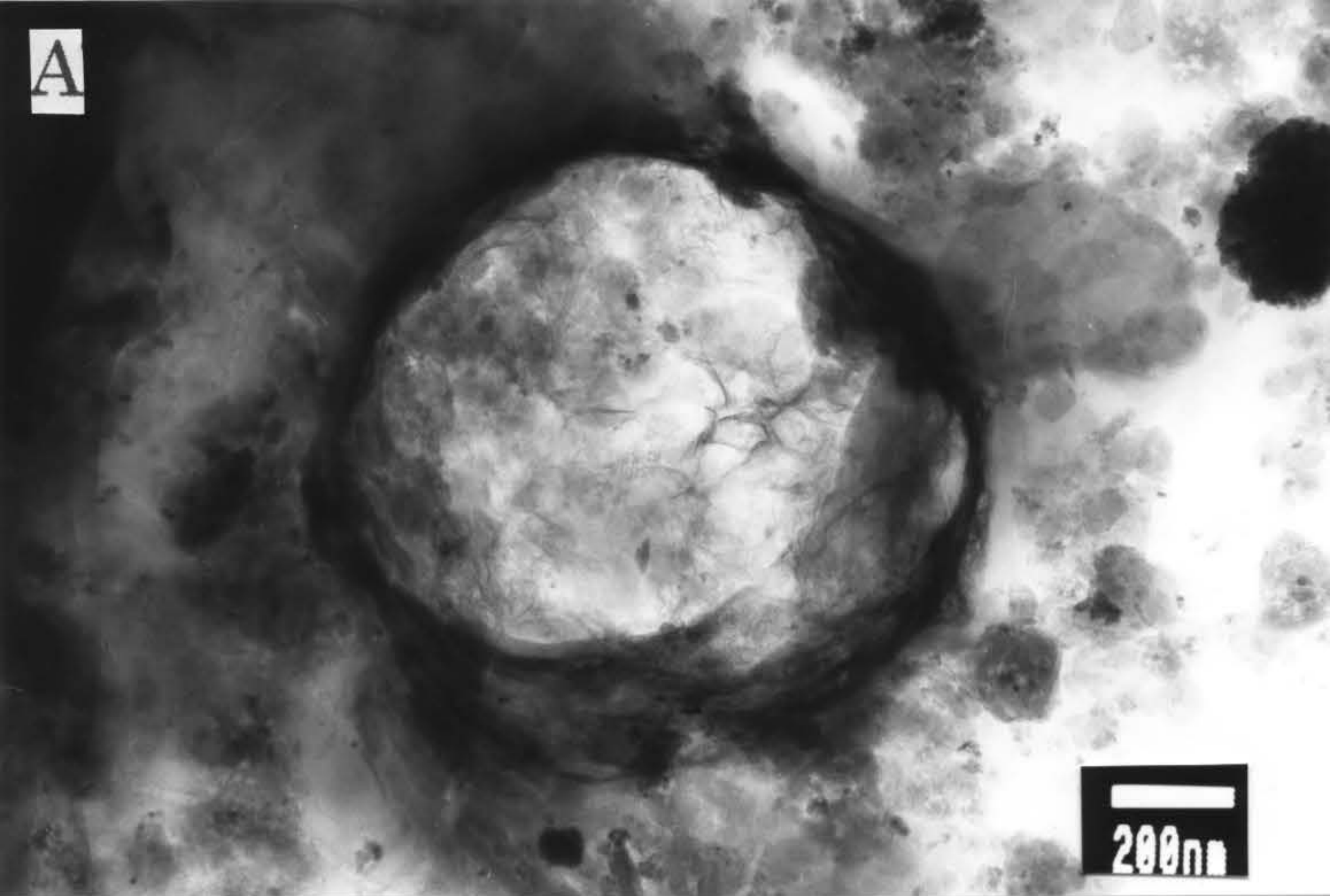
**B**

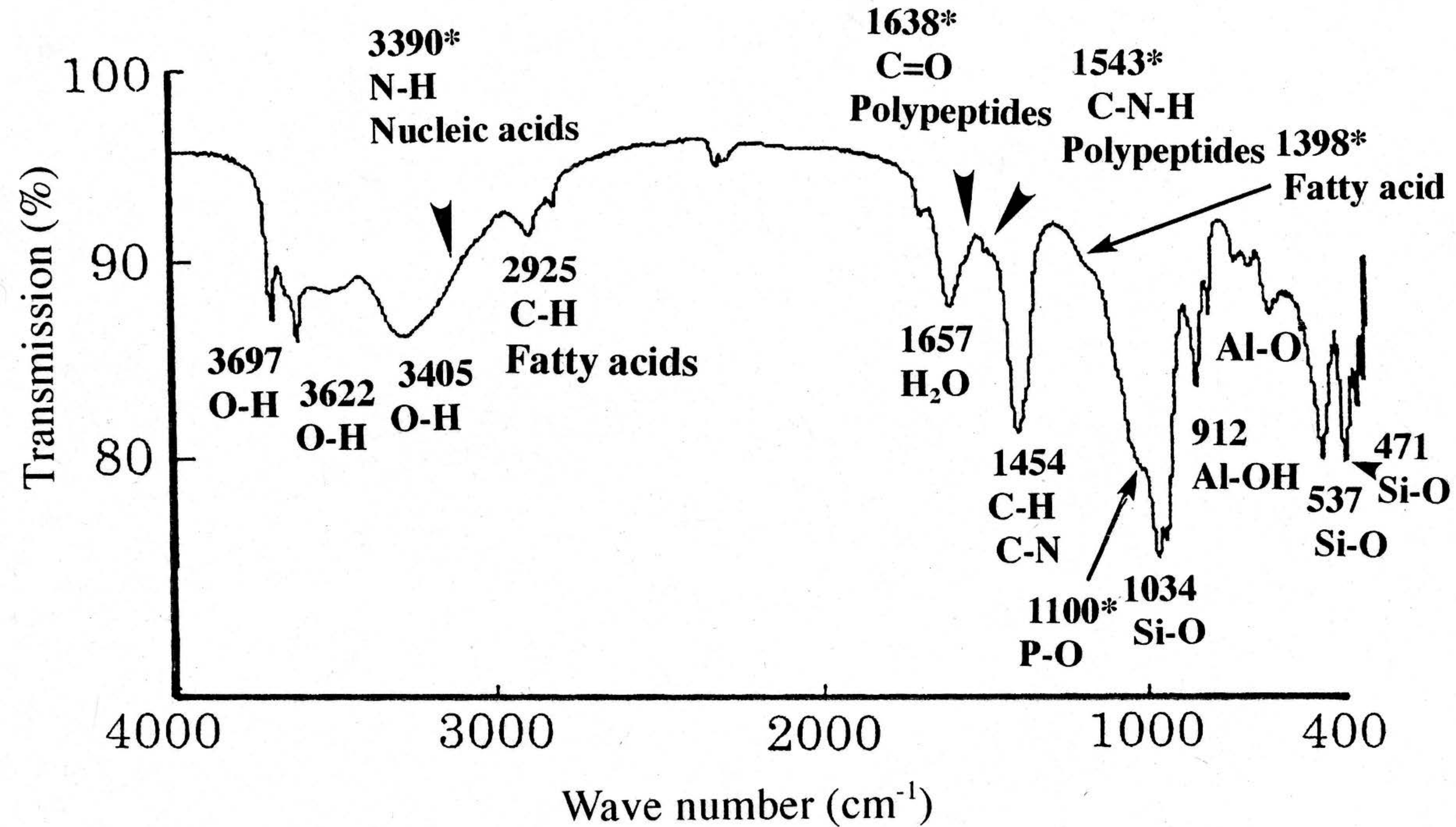
Halloysite

200 nm

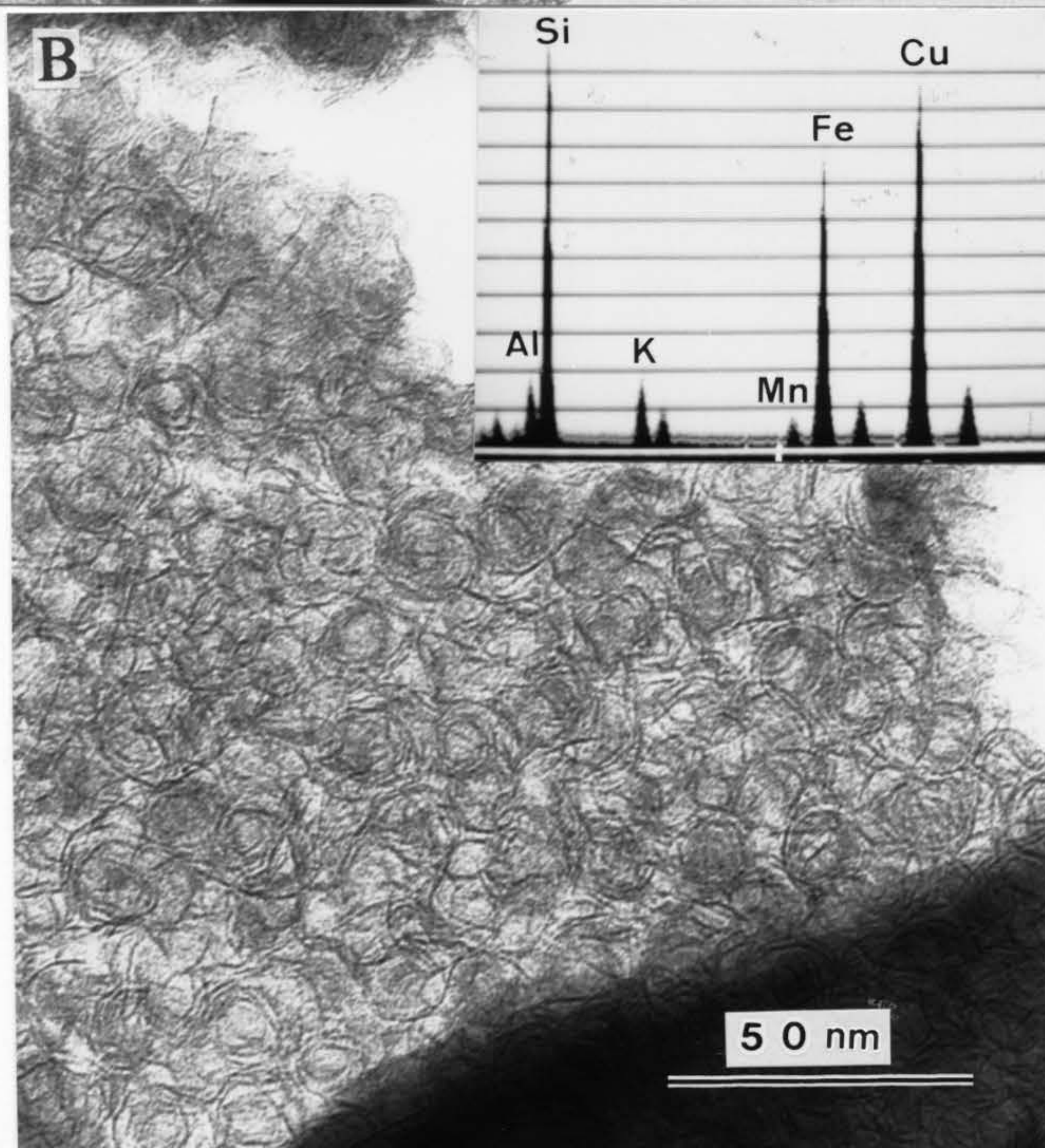
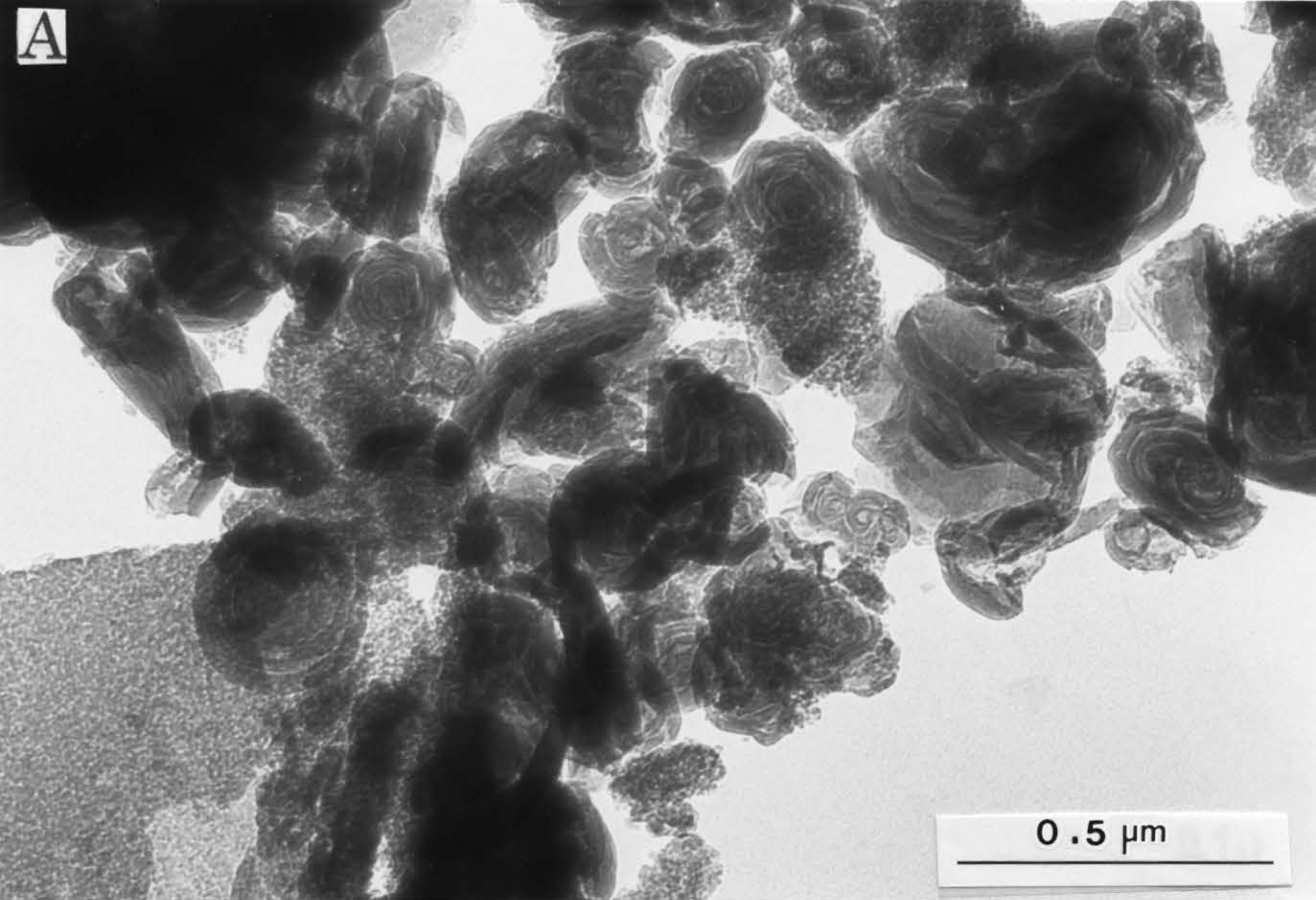
2.2 Å  
1.5 Å  
2.5 Å  
2.9 Å







\*Possible assignments after Filip and Hermann (2001)



Si-Al films on the adhesion surface

Bacterial cell

Si-O

Al-OH

Encapsulated surface

Degassing

Gas ( $\text{CO}_2$ ,  $\text{NO}_2$ )

Polypeptides  
Fatty acid  
Nucleic acids

Si-Al films

Swell out a skin eruption

Blow clay bubbles

Bacterial cell

Degassing

Cavity  
Vesicle

Bacterial cell

Vesicle containing clay

Vesicle

Swollen vesicle

500nm – 5 $\mu\text{m}$

Al, Si,  
S, Fe

Break out

Clay bubble

Cavity, Uniform Sphere

Blow clay bubbles

